Estuaries and Coasts
https://doi.org/10.1007/s12237-024-01384-1

RESILIENCE TO GLOBAL CHANGE IN SGOM

Variability of Dissolved Inorganic Carbon in the Most Extensive Karst Estuarine-Lagoon System of the Southern Gulf of Mexico

José Andrés Martínez-Trejo[1] · José Gilberto Cardoso-Mohedano[2] · Joan-Albert Sanchez-Cabeza[3] · José Martin Hernández Ayón[4] · Ana Carolina Ruiz-Fernández[3] · Mario Alejandro Gómez-Ponce[2] · Linda Barranco[5] · Daniel Pech[5]

Received: 4 December 2023 / Revised: 4 June 2024 / Accepted: 11 June 2024

Abstract

Coastal ecosystems with karstic geology have a unique characteristic where the dissolution of carbonate rocks can increase total alkalinity (TA) and dissolved inorganic carbon (DIC). This results in higher inorganic carbon budgets in coastal areas. One such ecosystem is the Terminos Lagoon, the most extensive tropical estuarine lagoon system in Mexico, located in the karstic aquifer of the Yucatan Peninsula and connected to the southern Gulf of Mexico (sGoM). We measured TA and DIC to evaluate the variability in Terminos Lagoon's of the carbonate system. We also estimated pH, partial CO_2 pressure (pCO_2), and aragonite saturation (Ω_{Ar}) along two transects from the main lagoon tributaries (Palizada and Candelaria rivers) to the coastal zone during the dry and rainy seasons. During the dry season, TA and DIC concentrations were significantly higher (3092 ± 452 µmol kg^{-1} TA, 2943 ± 522 µmol kg^{-1} DIC) than during the rainy season (2533 ± 228 µmol kg^{-1} TA, 2492 ± 259 DIC µmol kg^{-1}). Our calculations indicate that the rainy season pCO_2 (2532 ± 2371 µatm) seems higher than in the dry season (1534 ± 1192 µatm). This leads to a reduction in pH (7.9 ± 0.3 to 7.8 ± 0.3). These significant changes indicate that rain increases the flow of unsaturated river water into the lagoon. The results of this work contribute toward a dissolved inorganic carbon variability baseline in the sGoM and can be helpful to Terminos Lagoon decision-makers.

Keywords Ocean acidification · Carbonate system · Karst ecosystem · Estuarine Waters

Communicated by Wen-Chen Chou

✉ José Gilberto Cardoso-Mohedano
gcardoso@cmarl.unam.mx

1 Posgrado en Ciencias del Mar y Limnología, Universidad Nacional Autónoma de México, Avenida Ciudad Universitaria 3000, C.P. 04510, Coyoacán Ciudad de Mexico, México

2 Estación el Carmen, Instituto de Ciencias del Mar y Limnología, Universidad Nacional Autónoma de México, Carretera Carmen-Puerto Real km. 9.5, 24157 Ciudad del Carmen, Campeche, México

3 Unidad Académica Mazatlán, Instituto de Ciencias del Mar y Limnología, Universidad Nacional Autónoma de México, Avenida Joel Montes Camarena s/n , 82040 Mazatlán, Sinaloa, México

4 Instituto de Investigaciones Oceanológicas, Universidad Autónoma de Baja California, km. 103 Carretera Tijuana-Ensenada Ensenada, Baja California, México

5 Laboratorio de Biodiversidad Marina y Cambio Climático (BIOMARCCA), El Colegio de la Frontera Sur Lerma, 24500 Campeche, México

Introduction

Since the Industrial Revolution, anthropic activities have increased atmospheric CO_2 concentrations by ~40%, from 280 to > 410 ppm (IPCC 2020). This has also increased the concentration of marine CO_2 and dissolved inorganic carbon (DIC), increasing bicarbonates (HCO_3^-), and decreasing carbonates (CO_3^{2-}) and pH in seawater (Orr et al. 2018; Jiang et al. 2019). The extent of ocean acidification (Doney et al. 2009; Hofmann et al. 2019) is mainly controlled by seawater alkalinity, atmospheric CO_2 concentration, and $CaCO_3$ precipitation (Wang et al. 2013; Rosentreter and Eyre 2020). However, coastal ecosystems receive freshwaters, nutrients, and organic and inorganic inputs from the continental margins (Borges et al. 2006), causing more variability in the carbonate system than in the open ocean (Wallace et al. 2014; Cai et al. 2021). Thus, to evaluate acidification on continental margins, it is critical to assess the carbonate system variability in coastal ecosystems (Wallace et al. 2014; Doney et al. 2020; Barranco et al. 2022).

Published online: 10 July 2024

In coastal ecosystems, rivers are the primary source of organic and inorganic carbon reaching the continental shelf; this can be natural (e.g., allochthonous organic matter produced by photosynthesis, carbonate weathering) (Cai and Wang 1998; Cai 2003; Gomez et al. 2020) or be anthropogenic (e.g., industrial, agricultural, and urban wastewater) (Smith et al. 1999; Yang et al. 2015; Raymond and Hamilton 2018). Furthermore, riverine freshwaters can cause vertical and horizontal gradients in carbonate system parameters, dissolved oxygen, and salinity (Zopfi et al. 2001; Lee et al. 2015). Seasonality can also promote intra-annual variability of the carbonate system, causing high variability (Carstensen and Duarte 2019; Cai et al. 2021). Unlike the northern Gulf of Mexico (Wang et al. 2013; Gomez et al. 2020), studies of the carbonate system in the coastal ecosystems of the southern Gulf of Mexico (sGoM) are scarce (Osborne et al. 2022).

Karst, a landscape formed by carbonate (limestone, dolomite, marble) and evaporite rocks (gypsum, anhydrite, rock salt), covers up to 10% of the surface of Earth (Taminskas et al. 2006). The elevated CO_2 in the water column can increase the dissolution of carbonate, raising the HCO_3^- in the aquatic ecosystems (Eq. (1)) (Zhong et al. 2017; Han et al. 2018). Hence, karst aquatic ecosystems have higher total alkalinity (TA) and DIC (> 2500 µmol kg^{-1}) than marine waters (McGrath et al. 2019; Hu et al. 2022), increasing the inorganic carbon budgets in the coastal areas (Liu et al. 2019; Volta et al. 2020). Thus, evaluating the inorganic carbon system in coastal karst ecosystems is important.

$$CaCO_3 + CO_2 + H_2O \rightleftarrows Ca^{2+} + 2HCO_3^- \quad (1)$$

The Yucatan Peninsula, bordered by the sGoM and the Caribbean Sea, is a large karstic platform (165,000 km^2) (Bautista et al. 2011). The aquifer has intricate fractures, caves, and sinkholes (locally known as cenotes) (Perry et al. 2002). At the end of the Cretaceous period, a prominent asteroid hit the Yucatan Peninsula (Hildebrand et al. 1991), forming a circular alignment of karst sinkholes now named the Chicxulub ring of cenotes. This has caused a complex groundwater flow system and seawater intrusion, which reaches dozens of kilometers inland (Perry et al. 2002; Bauer-Gottwein et al. 2011). This groundwater system can export high DIC and TA waters (Gonneea et al. 2014) in the coastal area, causing DIC enrichment in the marine water column (Pain et al. 2020).

On the Yucatan Shelf, the carbonate system is driven by the interplay between oceanic water masses, influenced by the Yucatan upwelling (Merino 1997), and continental runoff, which are modulated by seasonal variations (Barranco et al. 2022). Due to the high TA and DIC values in the aquifer, their knowledge is fundamental to evaluating their influence on coastal lagoons and estuaries of the sGoM.

Terminos Lagoon (TL) is Mexico's most extensive tropical estuarine-lagoon system, connected with the sGoM through the Carmen and Puerto Real inlets (Yáñez-Arancibia & Day 1982). Because of its high biodiversity, the lagoon is classified as a Ramsar site (Ramsar 2004) and a Mexican Protected Area of Flora and Fauna (CONANP 1994). However, it is under high environmental pressure because of the impacts of the oil industry, land use change (Escobar-Toledo et al. 2017; Grenz et al. 2017), and untreated urban wastewater discharges from Ciudad del Carmen (191,238 pop.) (INEGI 2020). It receives freshwaters from (i) the Palizada River (70%), the main tributary of the Grijalva-Usumacinta River, the most extensive Mexican riverine system and the second-largest fluvial system of the GoM after the Mississippi-Atchafalaya river system (F. Vazquez et al. 2000; Fuentes-Yaco et al. 2001), and (ii) the Candelaria River (20%), also a karstic basin (Hudson et al. 2005; Álvarez-Pliego et al. 2015). This complexity of natural and anthropogenic influents may affect the lagoon's carbonate system, driving changes in the acidification of adjacent coastal zones and the sGoM.

In the present work, we evaluated the spatial and seasonal variation of the carbonate system, including DIC, TA, pH, partial CO_2 pressure (pCO_2), aragonite saturation (Ω_{Ar}), and [TA-DIC] from the Palizada and Candelaria rivers towards the coastal zone, during the rainy and dry seasons. The methodology and results of this work could contribute to understanding the inorganic carbon cycle in tropical estuarine systems, rivers, and karstic groundwaters worldwide and contribute to the knowledge of the impacts of coastal acidification in the sGoM.

Material and Methods

Study Area

Terminos Lagoon is in Campeche Bay (18°01′54″N, 90°59′15″W), has a 70 km length, 40 km maximum width, a surface area of 2500 km^2, and 3.0–3.5 m average depth (Medina-Gómez et al. 2015). The lagoon has a tropical island barrier system (Carmen Island), which has dry (March–May), rainy (June–October), and frontal winter storm (locally known as *Nortes*) seasons (November–February). Average evaporation is 1512 mm yr^{-1}, average precipitation is 1805 mm yr^{-1}, and the annual temperature ranges from 20 to 29 °C (David and Kjerfve 1998). The lagoon is subject to diurnal and semi-diurnal tidal regimes, and the residual circulation produces a net inflow of sGoM waters through the Puerto Real inlet and an outflow through the Carmen inlet (Ocaña and Lot

1996; Contreras Ruiz Esparza et al. 2014; Grenz et al. 2017). The lagoon receives 12.5×10^9 m^3 yr^{-1} of freshwater (Vazquez et al. 1999) from river discharge (95.42%), precipitation (4.55%), and groundwater (0.03%) (Herrera-Silveira et al. 2019). The Palizada (mean flow rate: 288 m^3 s^{-1}), Candelaria (72 m^3 s^{-1}), and Chumpan rivers (18 m^3 s^{-1}) are the main tributaries (Hudson et al. 2005; Medina-Gómez et al. 2015), with highest flow-rates in the rainy season (Cardoso-Mohedano et al. 2020).

Sampling

We sampled TL waters along two transects from the Palizada and Candelaria rivers to the coastal zone (Fig. 1, Table A1) during the dry (February 2020, March 2021) and rainy (November 2021) seasons. Each transect had nine stations, where we collected surface (0.5 m below the surface) and bottom (0.5 m above the bottom) water samples with a horizontal Van Dorn bottle.

To prevent CO_2 losses, we filled borosilicate glasses using a tube draining to the bottom of the glass, overflowing three times their volume. To minimize gas exchange with the atmosphere, we preserved the unfiltered water samples with mercuric chloride and sealed the glass with rubber and aluminum seals. The samples were then conserved in both light and darkness at a temperature of − 4 °C (Dickson et al. 2007). We measured in situ temperature (± 0.01 °C) and salinity (± 0.1) with a pre-calibrated EXO2 multiparameter sonde (YSI, 2020).

Carbonate System Analysis

In each water sample, we determined TA by a modified potentiometric titration method with a combined pH electrode, using 0.1 M HCl, in a custom-built closed cell (Hernández-Ayón et al. 1999). DIC was determined by coulometry (Johnson et al. 1987; CM5014, UIC, Joliet, USA). A Certified Reference Material (A. Dickson, Scripps, UCSD) was used for the DIC and TA measurements for a precision and accuracy of ± 3 µmol kg^{-1}. With TA, DIC, salinity, and temperature values, we calculated pH using the total pH scale, pCO_2, and Ω_{Ar}, with the PyCO2SYS 2.0 program (Humphreys et al. 2022), and using (Millero 2010) equations, which are valid in the ranges of 0 < temperature < 50 °C and 1 < salinity < 50.

In seawater, $[TA–DIC] = [CO_3^{2-}] - [CO_2]$ + Borate alkalinity. This parameter is conservative (independent of temperature and pressure), and it assists in evaluating processes such as mixing, biogeochemical reactions, and ocean acidification (Xue et al. 2018; Xue and Cai 2020). Thus, we calculated the apparent oxygen consumption (AOU) as the saturated oxygen concentration (McDougall and Barker 2011) minus the observed dissolved oxygen concentration. These calculations can be used as indicators

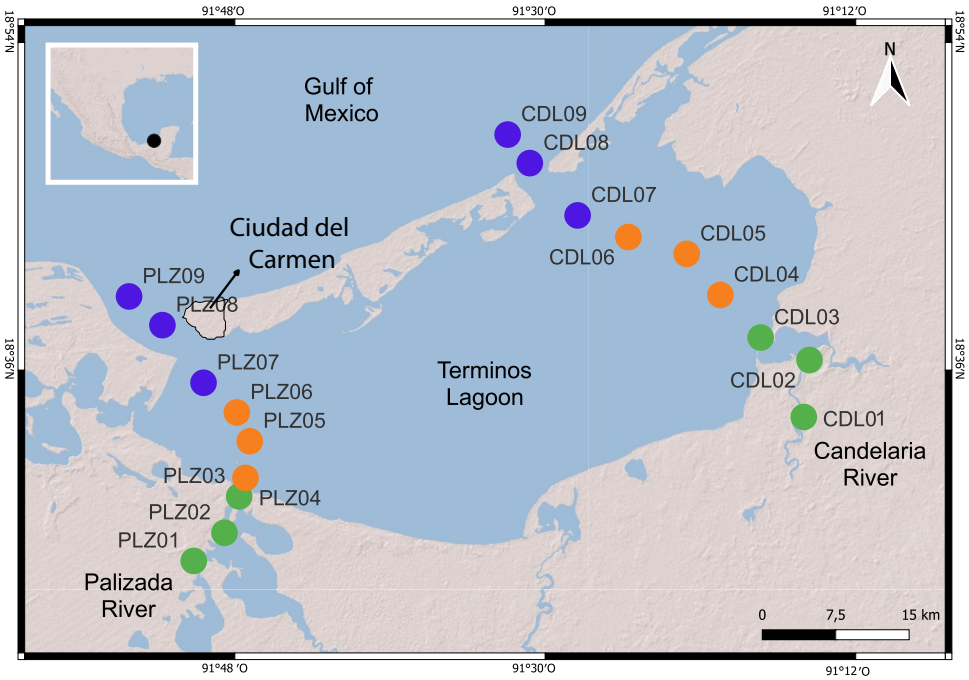

Fig. 1 Site map of Terminos Lagoon (southern Gulf of Mexico) includes sampling stations for Palizada and Candelaria estuaries and the studied areas: River (green), Estuarine (orange), and Coast (blue) areas. (For interpretation of the references to color in this Fig., the reader is referred to the web version of this article)

for carbonate biogeochemical processes (PyCO2SYS and Jupyter scripts, and raw data are included in the Supplementary Information).

Statistical Analyses

To evaluate the influence of Palizada and Candelaria rivers on the TL carbon system, we grouped the sampling stations into areas named (i) River, in the river courses, (ii) Estuarine, lagoon waters likely affected by river discharges, and (iii) Coast, near the lagoon inlets (Fig. 1, Table A1). The significance level for all analyses was set to $p < 0.05$. Since the variables did not show normal distributions (Shapiro–Wilk's test), we used Kruskal–Wallis and the post hoc Dun tests to evaluate differences between areas (River, Coast, and Estuarine) and Mann–Whitney tests to evaluate differences between seasons (dry and rainy), transects (Palizada and Candelaria) and depth (surface and bottom samples). For statistical analyses, we used the Python SciPy package 1.0 (Virtanen et al. 2020). To study the mixing process in the lagoon, we performed linear regressions using Ordinary Least Squares (OLS) regression with the Python statsmodels package 0.13.5 (Seabold and Perktold 2010).

Results

Salinity

During the dry season, the Candelaria Coast samples showed the most extensive salinity range (26.0–38.8). During the rainy season, the lowest ranges were in the Candelaria (0.4–7.6) and Palizada River samples (0.0–0.3; Table 1). Salinity differed significantly for the dry and the rainy season throughout the study area. Salinity showed

Table 1 Mean ± standard deviation (min–max) for salinity (S), pH, total alkalinity (TA) µmol kg^{-1}, dissolved inorganic carbon (DIC) µmol kg^{-1}, partial pressure of CO_2 (pCO_2) µatm and aragonite saturation (Ω_{Ar}) values in the study areas during the rainy and dry seasons

Areas	T° (C)	S	pH	TA (µmol kg^{-1})	DIC (µmol kg^{-1})	pCO_2 (µatm)	Ω_{Ar}
		Palizada					
		Dry					
River	26.5 ± 0.5 (25.5–27.2)	0.67 ± 0.81 (0–2.38)	7.8 ± 0.3 (7.5–8.5)	3332 ± 170 (3093–3512)	2627 ± 171 (3162–3636)	3255 ± 1422 (670–6129)	0.23 ± 0.19 (0–0.6)
Estuarine	26.4 ± 0.7 (25.6–27.8)	20 ± 11 (0.35–30.38)	7.84 ± 0.28 (7.4–8.4)	2980 ± 245 (2755–3483)	2872 ± 309 (2539–3456)	1425 ± 839 (623–3100)	1.9 ± 1.1 (0.4–3.5)
Coast	26.2 ± 0.5 (25.7–26.9)	28.52 ± 6.46 (17.13–36.02)	7.84 ± 0.16 (7.6–8)	2794 ± 89 (2635–2935)	2622 ± 84 (2501–2782)	1037 ± 381 (625–1717)	2.5 ± 0.7 (1.6–3.5)
		Rainy					
River	26.9 ± 0.2 (26.8–27.2)	0.18 ± 0.01 (0.17–0.19)	7.39 ± 0.09 (7.3–7.9)	2550 ± 89 (2430–2626)	2753 ± 130 (2581–2853)	6467 ± 1445 (4805–8129)	0.02 ± 0.01 (0.02–0.03)
Estuarine	27.2 ± 0.3 (26.9–27.7)	9.63 ± 9.22 (0.18–21.37)	7.74 ± 0.27 (7.4–8.0)	2462 ± 95 (2357–2611)	2444 ± 157 (2305–2665)	2441 ± 2361 (610–6040)	1.3 ± 1.2 (0.02–3.0)
Coast	27.3 ± 0.3 (26.9–27.6)	15.79 ± 10.12 (9.15–31.03)	7.84 ± 0.08 (7.7–8.8)	2392 ± 52 (2361–2484)	2319 ± 26 (2291–2348)	1067 ± 240 (874–1392)	1.5 ± 0.5 (1–2.2)
		Candelaria					
		Dry					
River	27.7 ± 1.2 (25.9–29.3)	11.88 ± 10.53 (0.7–28.06)	7.87 ± 0.23	3687 ± 580 (2849–4307)	3618 ± 647 (2745–4324)	1985 ± 1004 (711–3634)	1.8 ± 1.4 (0.6–5.2)
Estuarine	27 ± 1.1 (25.9–29.3)	25.26 ± 8.38 (8.94–33.89)	7.94 ± 0.15 (7.7–8.2)	2836 ± 87 (2682–3035)	2631 ± 111 (2392–2830)	833 ± 238 (518–1235)	2.9 ± 0.5 (2.3–3.8)
Coast	25.6 ± 0.8 (24.5–26.9)	33.76 ± 4.58 (26.0–38.8)	7.83 ± 0.11 (7.5–8.0)	2707 ± 153 (2500–2992)	2503 ± 151 (2289–2792)	902 ± 277 (668–1654)	2.7 ± 0.5 (1.5–3.2)
		Rainy					
River	26.9 ± 0.4 (26.6–27.5)	1.8 ± 3.22 (0.36–7.56)	7.62 ± 0.03 (7.6–7.7)	2783 ± 158 (2501–2865)	2878 ± 196 (2528–2973)	3514 ± 699 (2314–4140)	0.2 ± 0.3 (0.08–0.65)
Estuarine	27.5 ± 0.2 (27.4–27.8)	12.73 ± 5.97 (8.43–22.6)	7.94 ± 0.07 (7.8–8.0)	2435 ± 67 (2359–2542)	2333 ± 71 (2233–2425)	845 ± 72 (718–892)	1.8 ± 0.2 (1.6–2.0)
Coast	27.3 ± 0.4 (26.9–27.8)	28.33 ± 12.39 (12.52–38.56)	7.84 ± 0.08 (7.7–8.0)	2417 ± 6 (2412–2429)	2255 ± 82 (2152–2361)	909 ± 251 (625–1260)	2.1 ± 0.7 (1.3–2.9)

Table 2 Comparison of salinity and carbonate system variables between sampling areas (River, Estuarine, and Coast), transects (Candelaria and Palizada), and seasons (dry and rainy)

Variable	Factor	Tests		
Salinity	Season	W = 1549	$p = 0.003$	
	Transects	W = 1867	$p = 0.0002$	
	Depth	W = 1154	$p = 0.344$	
	Areas	$H = 52$	$p = 5.5 \times 10^{-12}$	
			River	***Estuarine***
		Estuarine	1.2×10^{-5}	-
		Coast	3.8×10^{-12}	0.007
TA	Season	W = 2138	$p = 8.7 \times 10^{-13}$	
	Transects	W = 1280	$p = 0.90$	
	Depth	W = 1258	$p = 0.80$	
	Areas	$H = 31$	$p = 2.0 \times 10^{-7}$	
			River	***Estuarine***
		Estuarine	0.0004	-
		Coast	1.8×10^{-7}	0.07
DIC	Season	W = 1804	$p = 1.9 \times 10^{-6}$	
	Transects	W = 1074	$p = 0.13$	
	Depth	W = 1305	$p = 0.95$	
	Areas	$H = 55$	$p = 1.3 \times 10^{-12}$	
			River	***Estuarine***
		Estuarine	1.4×10^{-6}	-
		Coast	1.7×10^{-12}	0.02
pCO_2	***River***	***Estuarine***		
	Season	W = 901	$p = 0.09$	
	Transects	W = 874	$p = 0.004$	
	Depth	W = 1440	$p = 0.34$	
	Areas	$H = 40$	$p = 2.5 \times 10^{-9}$	
			River	***Estuarine***
		Estuarine	2.8×10^{-7}	-
		Coast	7.2×10^{-8}	0.7
pH	Season	W = 1478	$p = 0.02$	
	Transects	W = 1608	$p = 0.04$	
	Depth	W = 1163	$p = 0.37$	
	Areas	$H = 8$	$p = 0.02$	
			River	***Estuarine***
		Estuarine	0.01	-
		Coast	0.12	0.36
Ω_{ar}	Season	W = 1628	$p = 0.0005$	
	Transects	W = 1836	$p = 0.0003$	
	Depth	W = 1173	$p = 0.41$	
	Areas	$H = 38$	$p = 4.7 \times 10^{-9}$	
			River	***Estuarine***
		Estuarine	6.9×10^{-7}	
		Coast	8.3×10^{-8}	0.6
[TA-DIC]	Season	W = 1601	$p = 8.4 \times 10^{-4}$	
	Transects	W = 1864	$p = 1.6 \times 10^{-4}$	
	Depth	W = 1134	$p = 0.28$	
	Areas	$H = 42$	$p = 9.9 \times 10^{-10}$	
			River	***Estuarine***
		Estuarine	2.8×10^{-7}	-
		Coast	4.1×10^{-9}	0.19

The W estimator corresponds to two-sample Mann-Whitney tests. The H indicates a Kruskal-Wallis test with its corresponding post hoc significance matrix below

significant differences between areas, with an increased (positive) gradient from River to Coast samples. Analysis post hoc indicated differences among the River, Coast, and Estuarine areas (Table 2). During the dry season, the Candelaria River stations showed a higher salinity variability (12 ± 11) than the Palizada River (0.7 ± 0.8), caused by the intrusion of saline waters only into the Candelaria River (Fig. 2a, b). As expected, salinity in the Candelaria transect was significantly higher than in the Palizada (Table 2) because the Palizada flow is four times larger.

TA

The highest TA range was observed in the Candelaria River area during the dry season (3685–4307 µmol kg^{-1}) and the lowest in the Palizada Estuarine and Coast areas (2357–2376 µmol kg^{-1}) during the rainy season (Table 1). TA during the dry season was significantly higher than during the rainy season throughout the study area. In both seasons, TA decreased along a gradient from the River to the Coast areas, showing significant differences. Analysis post hoc indicated that the River area differed significantly from both the Estuarine and Coast areas. The Estuarine samples did not differ from the Coast ones (Fig. 2c, d, Table 2). No significant differences were found between the Candelaria and Palizada transects. The OLS regression between Salinity and TA showed a weak relationship, although the result was statistically significant (p-value $= 9.09 \times 10^{-5}$, $r^2 = 0.134$; see Table A2, Fig. A1).

DIC

Similarly to TA, the highest DIC range (3667–4324 µmol kg^{-1}) was observed in the Candelaria River area during the dry season, and the lowest (2152–2258 µmol kg^{-1}) in the Candelaria Coast area during the rainy season (Table 1). The DIC values were significantly higher during the dry season than in the rainy season. In both seasons, the DIC decreased from the River to the Coast areas, showing significant differences. Analysis post hoc analysis indicated significant differences between the River, Coast, and Estuarine areas (Fig. 2e, f, Table 2). No significant differences were found between the Candelaria and Palizada transects. Between salinity and DIC a relationship, although moderate, was statistically significant (OLS regression, p-value $= 4.7 \times 10^{-10}$, $r^2 = 0.316$; see Table A3, Fig. A2). Between TA and DIC there was a strong and significant relationship (OLS regression, p-value $= 7.3 \times 10^{-58}$, $r^2 = 0.924$, Fig. 5; see Table A4).

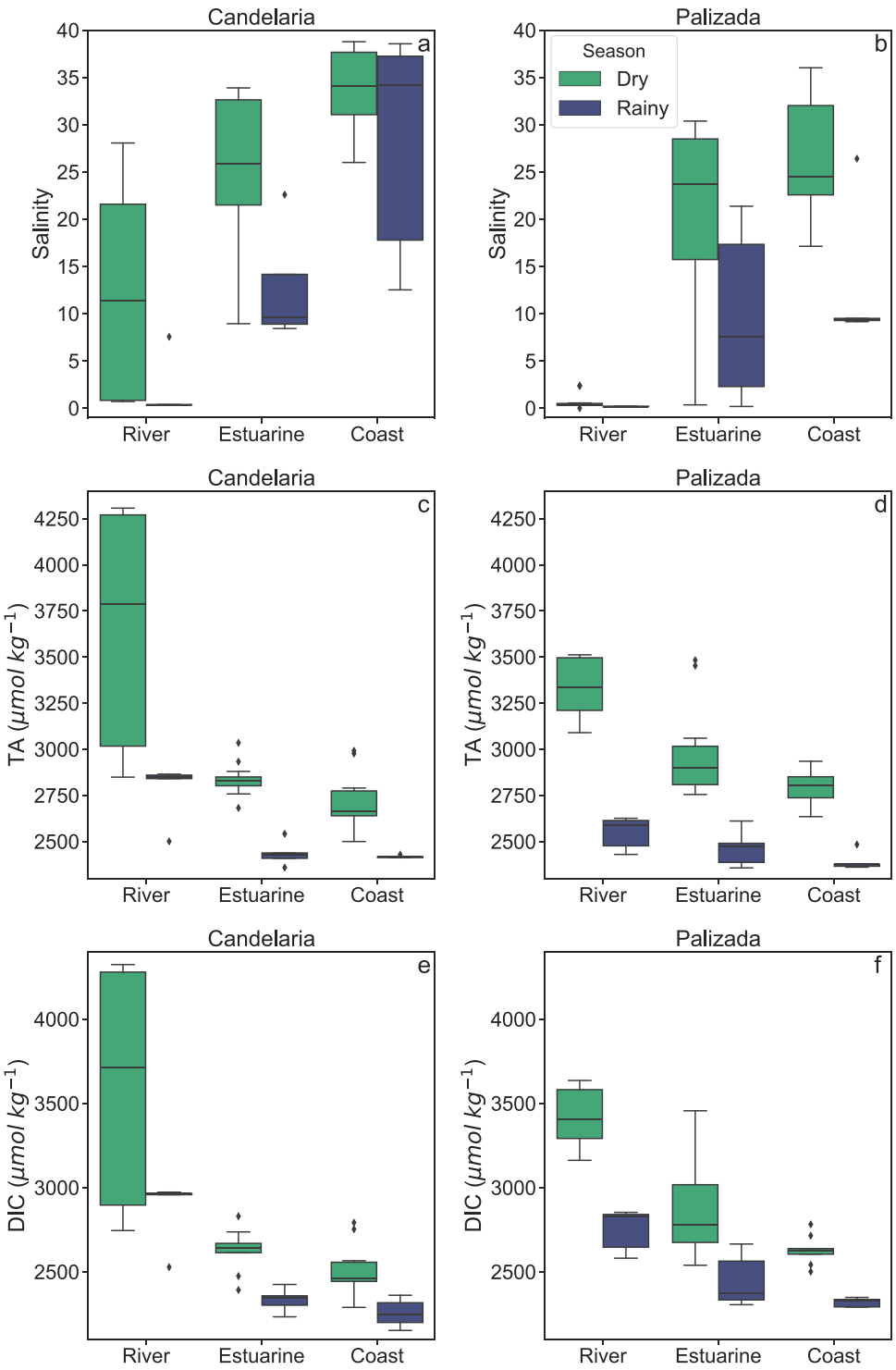

Fig. 2 Salinity, TA, and DIC concentrations for the Candelaria and Palizada transects by studied areas (River, Estuarine, and Coast) during the rainy and dry seasons. The boxes represent the interquartile range, the horizontal line within the boxes is the median, and the whiskers are the maximum and minimum values. Black dots represent the outliers. Terminos Lagoon, southern Gulf of Mexico

AOU

Palizada and Candelaria's transects had the lowest (negative) AOU values during the dry season. However, the Palizada River area showed positive AOU values (Fig. 3a, b). This suggests that most of the lagoon's primary productivity during the dry season increases water column DO. In contrast, in the Palizada River Area, dissolved oxygen consumption may occur due to the oxidation of organic matter caused by runoff. During the rainy season, the AOU values were consistently positive in the area, particularly in the Palizada River and Estuarine areas, causing the AOU values to be significantly higher than during the dry season (Table 2). This suggests that TL receives organic matter from river

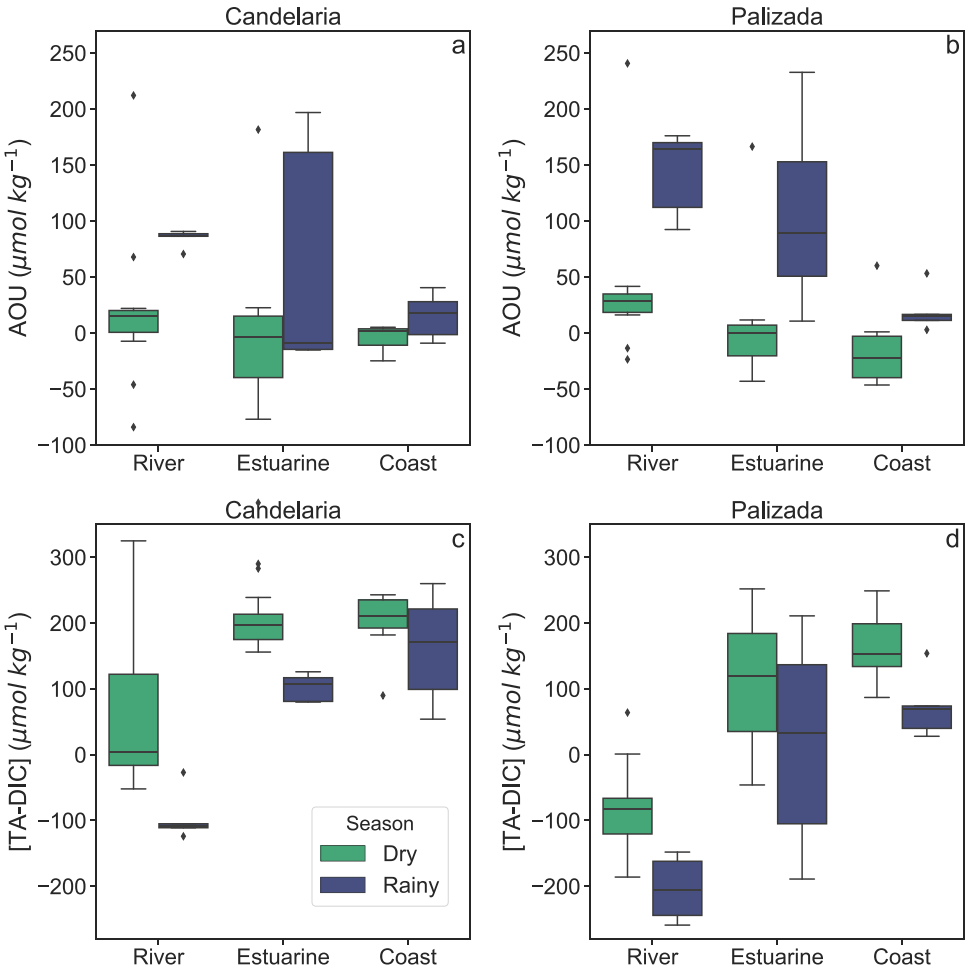

Fig. 3 AOU and [TA-DIC] concentrations for the Candelaria and Palizada transects by studied areas (River, Estuarine, and Coast) during the rainy and dry seasons. Terminos Lagoon, southern Gulf of Mexico

runoff, significantly increasing oxygen consumption during the rainy season.

pCO_2

The largest pCO_2 range (4805–8129 µatm) was recorded in the Palizada River area during the rainy season, and the lowest (518–596 µatm) in the Candelaria Estuarine area during the dry season (Table 1), with significant differences between transects. No significant differences were found between seasons. The pCO_2 decreased from the River to the Coast areas, showing significative differences between them. Analysis post hoc indicated that the River area showed significant differences from Estuarine and Coast areas, which did not differ between them (Fig. 4a, b, Table 2).

pH

The lowest pH range (7.3–7.5) was found in the Palizada River and Estuarine areas during the rainy season, and the highest range (8.0–8.5) was observed in the Palizada and Candelaria River and Estuarine areas during the dry season (Table 1). pH during the rainy season was significantly lower than during the dry one, and in the Palizada transect was significantly lower than in the Candelaria one. pH showed significant differences between areas. Analysis post hoc analysis revealed that the River areas showed significant differences from Estuarine and Coastal areas, which did not differ between them (Table 2, Fig. 4c, d).

Ω_{Ar}

Ω_{Ar} was supersaturated ($\Omega_{Ar} > 1$) in the Coast and Estuarine areas of both transects during both seasons and in the Candelaria River during the dry season. Ω_{Ar} was undersaturated ($\Omega_{Ar} < 1$) in the Palizada River area during both seasons and in the Candelaria River during the rainy season. The highest Ω_{Ar} range (3.5–5.2) was in the Candelaria River and Estuarine areas during the dry season, and the lowest range (0.00–0.03) was in the Palizada River area during the rainy season (Table 1). The Ω_{Ar} was significantly higher during the dry season than during the rainy season in the entire region. In the Candelaria transect, Ω_{Ar} was significantly higher than in the Palizada one (Table 2).

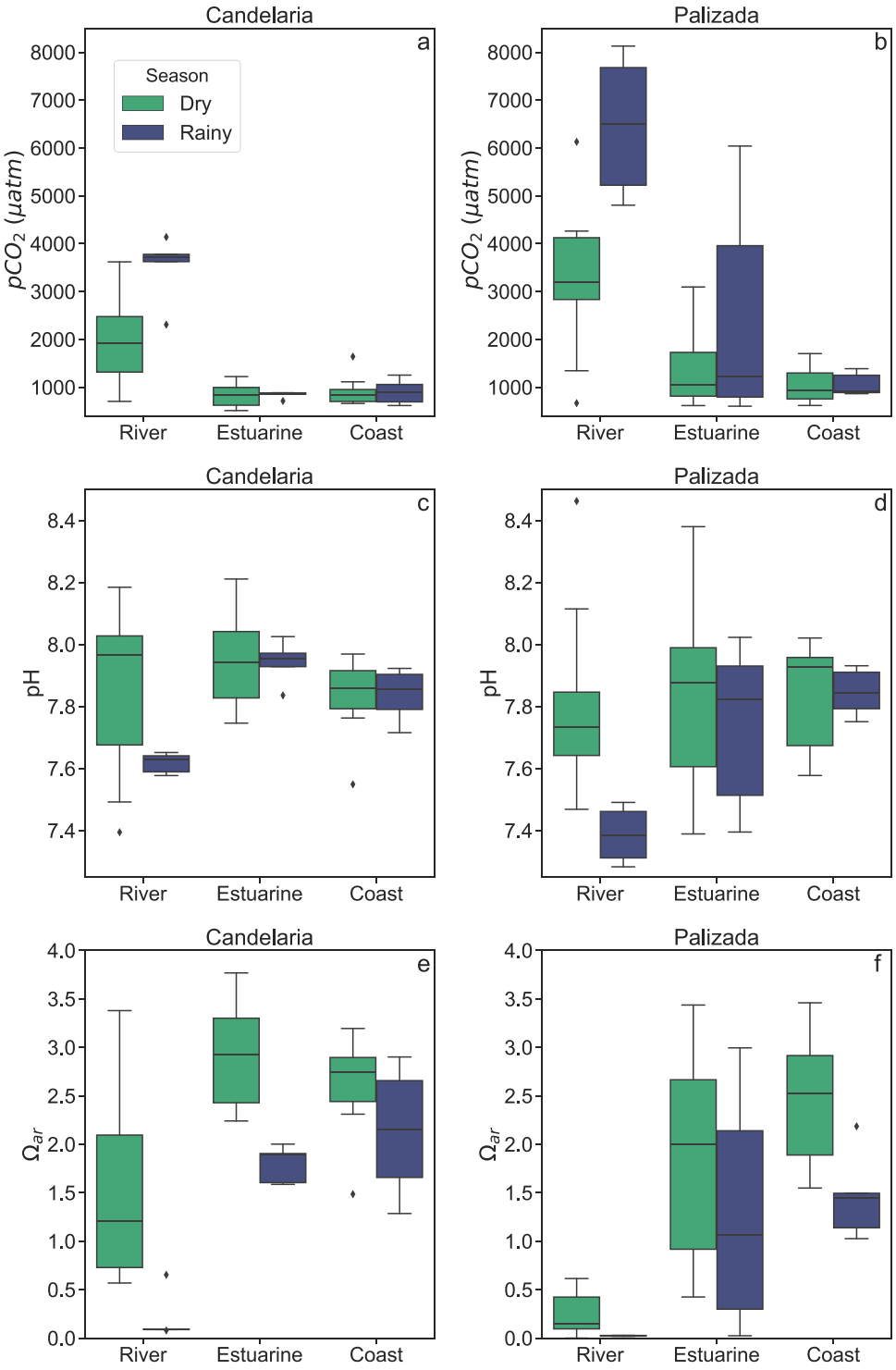

Fig. 4 pCO_2, pH, and Ω_{Ar} calculations result for the Candelaria and Palizada transects by studied areas (River, Estuarine, and Coast) during the rainy and dry seasons. Terminos Lagoon, southern Gulf of Mexico

Ω_{Ar} increased from the Rivers to the Coast areas. Analysis post hoc indicated that the River area differed significantly between the Estuarine and the Coast areas, but the Estuarine samples did not differ from the Coast ones (Fig. 4e, f, Table 2).

[TA-DIC]

The highest levels of [TA-DIC] were observed in the Candelaria River area during the dry season, while the lowest levels were recorded in the Palizada River area during the rainy season.

Throughout the study area, [TA-DIC] levels were significantly lower during the rainy season than during the dry season. [TA-DIC] values in the Candelaria transect were significantly higher than in the Palizada transect. Analysis post hoc indicated that the River area differed significantly from the Estuarine and the Coast, which did not differ among them (Fig. 3c, d, Table 2).

Discussion

Terminos Lagoon Carbonate System

TA and DIC did not reveal a perfect conservative behavior with salinity (Figs. A1, A2), presumably owing to the complexity of this lagoon-estuarine system and its exchanges with marine and terrestrial sources. However, the correlation between TA and DIC in the whole area was significant (Fig. 5; $r^2 = 0.924$, $p < 0.05$; Table A4). It appears that the TL inorganic carbon system in this lagoon is primarily influenced by the equilibrium of the carbonate system, despite the possible existence of various carbon sources and potential disturbances from unfiltered materials in the water samples, such as organic matter or resuspended carbonate sediments.

Averaged over space and time, TL was 2885 ± 460 µmol kg^{-1} TA and DIC 2808 ± 506 µmol kg^{-1}, higher than on the Yucatan Shelf (2388 ± 11 µmol kg^{-1} TA, 2047 ± 16 µmol kg^{-1} DIC (Barranco et al. 2022)) but lower than for the Yucatan karst aquifer (3000–8000 µmol kg^{-1} TA; Gonneea et al. 2014, 5900-–8000 µmol kg^{-1} DIC; Pain et al. 2020). Although the lagoon receives marine waters from the sGoM, it is clearly affected by karst waters.

During the dry season, TA (3067 ± 456 µmol kg^{-1}) and DIC (2957 ± 527 µmol kg^{-1}) were significantly higher than during the rainy season (TA 2503 ± 154 µmol kg^{-1}, DIC 2496 ± 262 µmol kg^{-1}), indicating that TL receives predominantly karst waters during the dry season (Fig. 2c–f). On the contrary, during the rainy season, freshwater inputs seem to reduce the lagoon karstic conditions because, although surface waters receive TIC and DIC-enriched waters (Fig. 6), freshwater inputs reduce these concentrations (Guo et al. 2008; Akhtar et al. 2021). pCO_2 tended to be higher during the rainy (2607 ± 2366 µatm) than during the dry season (1596 ± 1178 µatm, Fig. 3a, b, 6). During the dry season, [TA-DIC] values were significantly reduced, reaching negative values, mainly in the river areas (Fig. 3c, d). In these conditions, the AOU values showed positive values, indicating high oxygen consumption (Fig. 3a, b). River basins can receive high amounts of organic matter, which increases dissolved CO_2 when oxidized, causing a higher concentration of pCO_2 in estuarine ecosystems than the adjacent marine waters (Cai 2003; Gaspar et al. 2018; Abril et al. 2021), which can be enhanced during the rainy season owing to increased runoff (Sarma et al. 2012; Dutta et al. 2019).

Our study suggests that river runoff increases the organic matter in the water column during the rainy season in TL. This organic matter is oxidized, reducing the water's dissolved oxygen. As a result, CO_2 inputs from rivers, likely

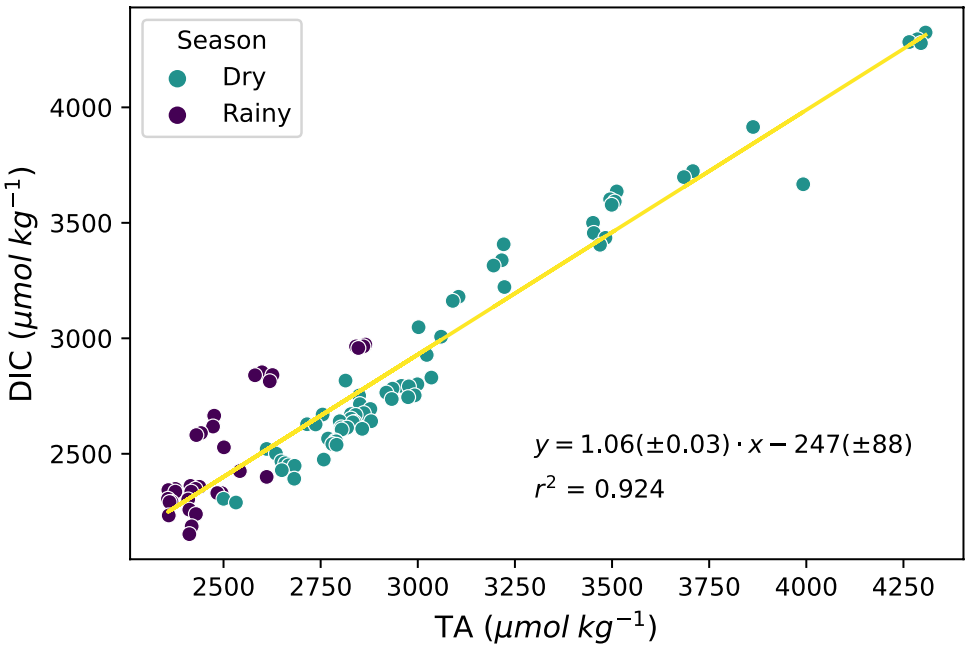

Fig. 5 Scatterplot and linear regression of DIC vs TA concentrations. Terminos Lagoon, southern Gulf of Mexico

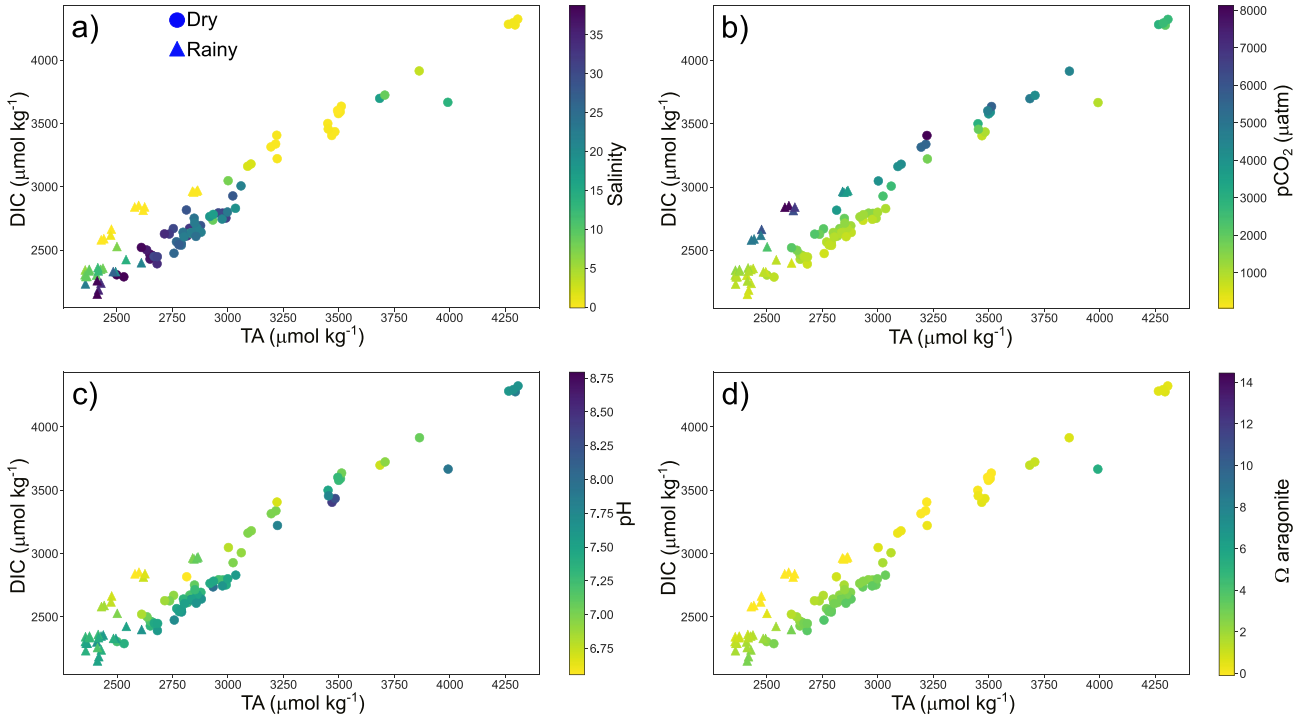

Fig. 6 DIC vs TA, salinity, pCO_2, pH, and ΩAr during dry and rainy seasons. Terminos Lagoon, southern Gulf of Mexico

due to the degradation of organic matter, increase, causing a significant pH decrease from 7.9 ± 0.2 during the dry season to 7.7 ± 0.2 during the rainy season (Fig. 4c, d).

This pH decrease seems to lead to a reduction in Ω_{Ar}, which drops from 2.4 ± 2.5 during the dry season to 1.5 ± 2.5 during the rainy season (Fig. 4e, f) throughout the study area. However, during the rainy season, the Ω_{Ar} presented values less than one in river areas. Aragonite saturation is calculated using the following equation (Mucci 1983):

$$\Omega_{ar} = \frac{[Ca^{2+}][CO_2^{2-}]}{K_{sp}}$$

where, $[Ca^{2+}]$ is the calcium concentration determined in CO2sys (Lewis and Wallace 1998) according to a linear relationship with salinity (Culkin 1965; Takahashi et al. 1982). Indeed, we observe a significant linear relationship between salinity and Ω_{Ar} for salinities below 25 (Fig. A3, $r^2 = 0.716$), but the intercept (0.265 ± 0.001) is not zero, as expected for karstic freshwaters. This result highlights the limitations of the conventional method of calculating aragonite saturation in karst estuaries.

To explore the possible effects of river waters on the TL carbonate system, we defined three types of waters according to their salinity range: river (0–1), estuarine (1–15), and coastal (15–39) waters. The relationship between [TA-DIC] and pH for each water type indicates that river waters show significant linear relationships ($p = 4.7 \times 10^{-19}$, $r^2 = 0.955$). The lowest values of [TA-DIC] were in the river waters, suggesting higher CO_2 concentrations, leading to the lowest pH values in the study area (Figs. 7 and 8). [TA–DIC] and pH in estuarine and coastal waters also showed significant relationships ($p = 1.8 \times 10^{-9}$, $r^2 = 0.857$; $p = 4.2 \times 10^{-19}$, $r^2 = 0.794$, respectively). In these waters, [TA-DIC] were predominantly positive, indicating high $[CO_3^{2-}]$ inputs to the lagoon, and a high calcium concentration is expected since the TL is a karst ecosystem. Hence, despite the potential presence of multiple carbon sources and possible perturbations from unfiltered materials, such as organic matter or resuspended carbonate particles, the TL inorganic carbon system appears mainly driven by the carbonate system equilibrium.

Estuarine Carbonate Variations

During the dry season, when freshwaters discharge is lowest, the innermost stations of the Candelaria River area (CDL01-02) had the highest TA (3685–4307 µmol kg^{-1}) and DIC (3667–4324 µmol kg^{-1}), and also showed seawater intrusion (salinity range: 0.7–28.1). High TA and DIC could be caused by (i) karstic groundwater discharge enriched in TA and DIC (Liu et al. 2019), (ii) seawater intrusion, which can increase the water residence time that facilitates the dissolution of carbonates, and (iii) high temperatures, which raise evaporation, leading to higher concentrations of TA and DIC.

Similarly, during the dry season, the stations under the influence of the Palizada River (PLZ01-04) had high TA (3495–3512 µmol kg^{-1}) and DIC (3578–3636 µmol kg^{-1}),

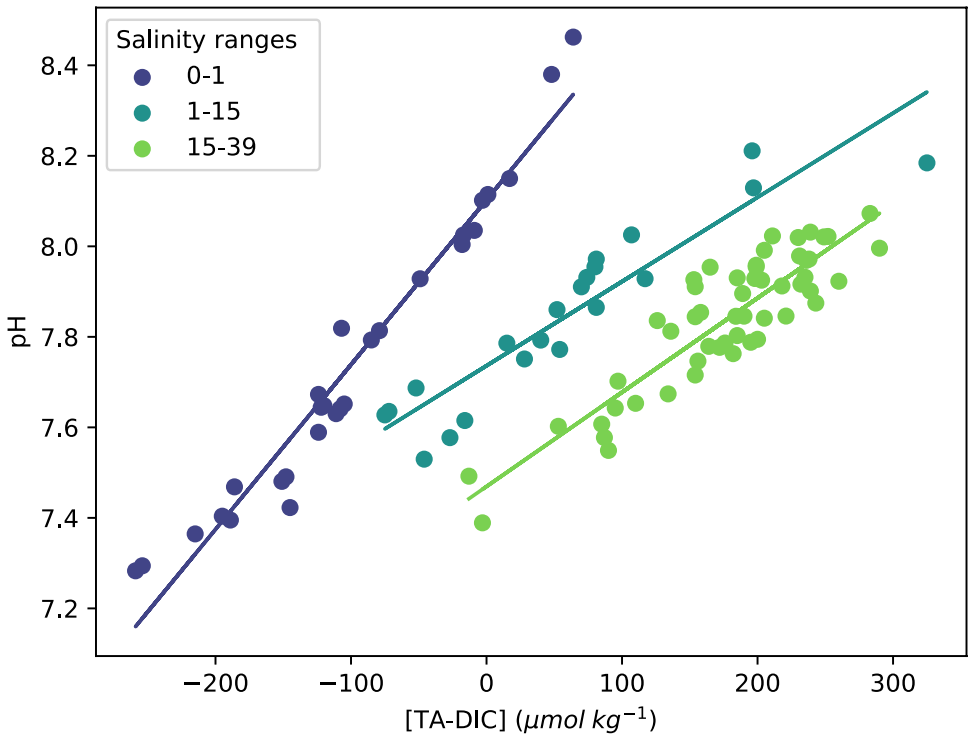

Fig. 7 Relationship between [TA-DIC] and pH and TA across Different Salinity Ranges. Terminos Lagoon, southern Gulf of Mexico

also indicating the influence of karst waters. However, TA and DIC were higher at the Candelaria than at the Palizada estuary (Fig. 2c–f). On the one hand, the Palizada River receives more freshwaters that dissolves the carbonate species water concentrations and, on the other hand, the Candelaria basin is closer to the Yucatan Peninsula (Ramos 1975; Gunn et al. 1995), receiving more karstic waters enriched in TA and DIC. Thus, the differences in carbonate species concentrations between the rivers may be caused by the relative amounts of freshwaters and karstic waters they receive.

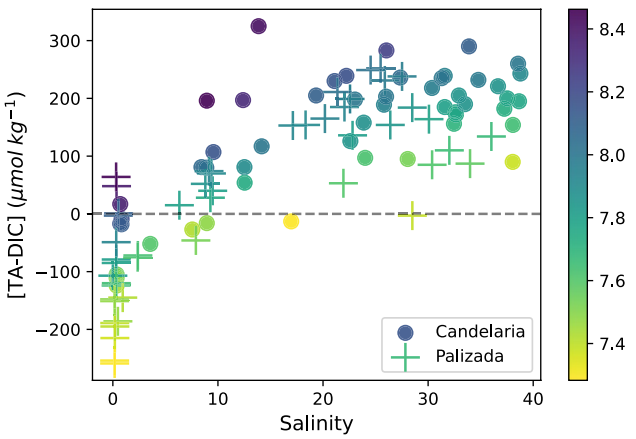

Fig. 8 Scatterplot of salinity vs [TA-DIC]. The color bar indicates pH. Terminos Lagoon, southern Gulf of Mexico

Hence, the river flow seasonality is crucial in controlling the TL carbonate system.

During the rainy season, the Palizada River had dissolved oxygen depletion conditions (AOU positively values) and consistently negative [TA-DIC] (Fig. 3), suggesting that runoff increases CO_2 concentrations in the river waters, causing the highest pCO_2 levels (6040–8129 µatm) in the studied area. These levels are higher than those of the Mississippi-Atchafalaya system in the Gulf of Mexico (370–2000 µatm; Cai 2003) and other rivers worldwide (200 to 4000 µatm; Cole et al. 2007; Raymond et al. 2013; Araujo et al. 2019). Rivers with pCO_2 values exceeding 3000 µatm generally have elevated organic matter concentrations (Reyes and Merino 1991; Araujo et al. 2019). Tropical soils have high organic matter concentrations that produce CO_2 when oxidized. In contact with moisture, organic matter creates H_2CO_3 that dissolves carbonate rocks in the epikarst zone. This leads to slow percolation flows through cracks and fissures to the phreatic area, causing oversaturation, $CaCO_3$ precipitation, and CO_2 release into caves and fractures (Class et al. 2021; Jaqueto et al. 2021). During the rainy season, the Grijalva-Usumacinta River basin's high rainfall (Cardoso-Mohedano et al. 2022) may release accumulated CO_2 from the aquifer into the river basin. The sum of lithogenic and organic CO_2 could explain high pCO_2 concentrations in the Palizada River. The higher CO_2 levels in the Palizada River area decrease the pH during both seasons (pH 7.8 ± 0.3 dry season, 7.39 ± 0.09 rainy season).

On the other hand, the Candelaria River area had the highest [TA-DIC] values during the dry season. In these

conditions, the dissolved oxygen levels do not indicate respiration or photosynthesis processes (AOU values are close to zero). This suggests a high CO_3^{2-} input in the Candelaria River area, possibly due to the dissolution of $CaCO_3$ (Xue and Cai 2020) from carbonate rocks. This confirms that the Candelaria River had more karstic conditions than the Palizada River.

Resilience of Terminos Lagoon to Coastal Acidification

Biota of estuarine ecosystems is adapted to salinity and pH river-coast gradients (Sosa-López et al. 2006; García-Ríos et al. 2013; Grenz et al. 2017), and in TL the foraminifera assemblages follow the lagoon circulation and the river's plume distribution (Phleger and Ayala 1971). Although TL had saturated conditions, a pH decrease on the continental shelf caused by ocean acidification (Orr et al. 2005; Hoegh-Guldberg et al. 2007) added to other anthropogenic impacts on the lagoon (Queb-Suarez et al. 2022; Celis-Hernandez et al. 2023; Jupin et al. 2023), could stress the TL ecosystem (Vinebrooke et al. 2004; Grenier et al. 2020; Kibria et al. 2021).

The Palizada and Candelaria rivers presented the highest pCO_2 levels. So, in an increased atmospheric CO_2 scenario, the pH of river waters could remain relatively stable. In contrast, the coastal areas presented lower pCO_2 levels, so increased atmospheric CO_2 can significantly reduce pH in coastal regions. This process could reduce the river-coastal pH gradient in the TL estuaries, thereby causing the displacement of organisms towards the coast, where salinity is higher. This could limit organisms' potential habitat and osmoregulatory capacity to estuaries' extreme pH and salinity conditions (Freitas et al. 2017; Liu et al. 2024). Urban discharges from Ciudad del Carmen could further restrict the organisms' habitat to the northwestern TL, increasing their vulnerability. Thus, decreasing untreated wastewater discharges from Ciudad del Carmen to the aquatic ecosystems could help improve the TL's resilience to coastal acidification.

Our results indicate that river freshwaters raise CO_2 water concentrations, thereby reducing pH values, mainly in the Palizada River area. Although TL had supersaturated Ω_{Ar} throughout the lagoon, the Palizada estuary and its coastal zone of influence can be the most vulnerable TL area to acidification effects. During the rainy season, rivers increase the CO_2 discharge to the coastal zone. Furthermore, industrial activities and urban wastewater increase organic matter in the sGoM rivers (Herrera-Silveira et al. 2019; Machain-Castillo et al. 2020; Cardoso-Mohedano et al. 2022) that, when oxidized, can increase CO_2 concentration in the water, contributing to coastal acidification. Our results indicate that, when receiving high CO_2 loads from natural or anthropic sources, karst estuaries can displace the carbonate system's equilibrium, increasing the CO_2 concentration in the water column. Considering sea level rise acceleration in the Yucatan Peninsula (Carnero-Bravo et al. 2016; Ruiz-Fernández et al. 2020), which can increase marine intrusion into karst aquifers (Liu et al. 2019), added to an increased amount of anthropogenic organic matter inputs (Moreno-Pérez et al. 2021; Cohuo et al. 2023), the flow of carbon from the Yucatan Peninsula to the sGoM may increase, thus enhancing ocean acidification. Implementing management programs that decrease organic matter and nutrient concentrations in rivers and aquifers that discharge to the coastal zone can help to increase the sGoM resilience to ocean and coastal acidification.

In summary, the results indicate that the equilibrium of the carbonate system drives the Terminos Lagoon inorganic carbon system, which is influenced by karst and river water inflows. During the dry season, the lagoon receives mainly karst waters, resulting in higher concentrations of TA and DIC. Freshwater inputs reduce these concentrations during the rainy season and decrease the lagoon's karstic conditions. The rainy season also brings increased CO_2 inputs from rivers, lowering pH in the Palizada River-influenced area. The results of this work contribute towards a dissolved inorganic carbon variability baseline in the sGoM coastal ecosystems and can be helpful to Terminos Lagoon decision-makers.

Supplementary Information The online version contains supplementary material available at https://doi.org/10.1007/s12237-024-01384-1.

Funding This work was partially supported by the projects: "Programa de Apoyo a Proyectos de Investigación e Innovación Tecnológica," Universidad Nacional Autónoma de México (PAPIIT IA101821); ICML-UNAM Influence of the COVID-19 pandemic on the Terminos lagoon. The support of Posgrado en Ciencias del Mar y Limnologia - UNAM and a Ph.D. fellowship from El Consejo Nacional de Humanidades, Ciencias y Tecnología-Mexico (CONACYT, CVU: 666631) are acknowledged by Martínez-Trejo J. A. Special thanks to J.A. Reda Deara, H. Alvarez Guillen (for sampling work), L. F. Álvarez-Sánchez (for data curation), and Ann Grant for editing the manuscript for English and overall contents.This is a contribution from the Research Network of Marine-Coastal Stressors in Latin America and the Caribbean (REMARCO).

Code and Data Availability The raw data can be consulted from the RU-ICML University Repository: https://metadata.icmyl.unam.mx/handle/20.500.12201/11367. The Python scripts and raw data can be consulted in: https://github.com/gilbertoCM/terminos-lagoon-carbonate.git.

References

Abril, G., B.G. Libardoni, N. Brandini, L.C. Cotovicz, P.R.P. Medeiros, G.H. Cavalcante, and B.A. Knoppers. 2021. Thermodynamic uptake of atmospheric CO2 in the oligotrophic and semiarid São Francisco estuary (NE Brazil). *Marine Chemistry* 233: 103983. https://doi.org/10.1016/j.marchem.2021.103983.

Akhtar, S., Sk Md. Equeenuddin, and F. Bastia. 2021. Distribution of pCO2 and air-sea CO2 flux in Devi estuary, eastern India. *Applied Geochemistry* 131: 105003. https://doi.org/10.1016/j.apgeochem.2021.105003.

Álvarez-Pliego, N., A.J. Sánchez, R. Florido, and M.Á. Salcedo. 2015. First record of South American suckermouth armored catfishes (Loricariidae, Pterygoplichthys spp.) in the Chumpan River system, southeast Mexico. *BioInvasions Records* 4: 309–314. https://doi.org/10.3391/bir.2015.4.4.14.

Araujo, M., C. Noriega, C. Medeiros, N. Lefèvre, J.S.P. Ibánhez, M. Flores Montes, A.C. da Silva, and M. de L. Santos. 2019. On the variability in the CO2 system and water productivity in the western tropical Atlantic off North and Northeast Brazil. *Journal of Marine Systems* 189. Elsevier: 62–77. https://doi.org/10.1016/J.JMARSYS.2018.09.008.

Barranco, L.M., J. Martín Hernández Ayón, D. Pech, C. Enriquez, J. Herrera, I. Mariño, and J. Carlos Herguera. 2022. Physical and biogeochemical controls of the carbonate system of the Yucatan Shelf. *Continental Shelf Research* 244. Pergamon: 104807. https://doi.org/10.1016/J.CSR.2022.104807.

Bauer-Gottwein, P., B.R.N. Gondwe, G. Charvet, L.E. Marín, M. Rebolledo-Vieyra, and G. Merediz-Alonso. 2011. Review: The Yucatán Peninsula karst aquifer, Mexico. *Hydrogeology Journal* 19: 507–524. https://doi.org/10.1007/s10040-010-0699-5.

Bautista, F., G. Palacio-Aponte, P. Quintana, and J.A. Zinck. 2011. Spatial distribution and development of soils in tropical karst areas from the Peninsula of Yucatan, Mexico. *Geomorphology* 135: 308–321. https://doi.org/10.1016/j.geomorph.2011.02.014.

Borges, A.V., L.-S. Schiettecatte, G. Abril, B. Delille, and F. Gazeau. 2006. Carbon dioxide in European coastal waters. *Estuarine, Coastal and Shelf Science* 70: 375–387. https://doi.org/10.1016/j.ecss.2006.05.046.

Cai, W.J. 2003. Riverine inorganic carbon flux and rate of biological uptake in the Mississippi River plume. *Geophysical Research Letters* 30. https://doi.org/10.1029/2002GL016312.

Cai, W.J., R.A. Feely, J.M. Testa, M. Li, W. Evans, S.R. Alin, Y.-Y. Xu, et al. 2021. Natural and anthropogenic drivers of acidification in large estuaries. *Annual Review of Marine Science* 13: 23–55. https://doi.org/10.1146/annurev-marine-010419-011004.

Cai, W.J., and Y. Wang. 1998. The chemistry, fluxes, and sources of carbon dioxide in the estuarine waters of the Satilla and Altamaha Rivers, Georgia. *Limnology and Oceanography* 43: 657–668. https://doi.org/10.4319/lo.1998.43.4.0657.

Cardoso-Mohedano, J.G., J.C. Canales-Delgadillo, M.L. Machain-Castillo, J.G. Hernández-Hernández, J.A. Sanchez-Cabeza, A.C. Ruiz-Fernández, R. Alonso-Rodríguez, et al. 2020. Absence of hypoxia events in the adjacent coastal waters of Grijalva-Usumacinta river, Southern Gulf of Mexico. *Marine Pollution Bulletin* 156. Elsevier Ltd: 111174. https://doi.org/10.1016/j.marpolbul.2020.111174.

Cardoso-Mohedano, J.G., J.C. Canales-Delgadillo, M.-L. Machain-Castillo, W.-N. Sanchez-Muñoz, J.-A. Sanchez-Cabeza, K. Esqueda-Lara, M.A. Gómez-Ponce, et al. 2022. Contrasting nutrient distributions during dry and rainy seasons in coastal waters of the southern Gulf of Mexico driven by the Grijalva-Usumacinta River discharges. *Marine Pollution Bulletin* 178: 113584. https://doi.org/10.1016/j.marpolbul.2022.113584.

Carnero-Bravo, V., J.-A. Sanchez-Cabeza, A.C. Ruiz-Fernández, M. Merino-Ibarra, C. Hillaire-Marcel, J.A. Corcho-Alvarado, S. Röllin, M. Diaz-Asencio, J.-G. Cardoso-Mohedano, and J. Zavala-Hidalgo. 2016. Sedimentary records of recent sea level rise and acceleration in the Yucatan Peninsula. *Science of the Total Environment* 573: 1063–1069. https://doi.org/10.1016/j.scitotenv.2016.08.142.

Carstensen, J., and C.M. Duarte. 2019. Drivers of pH variability in coastal ecosystems. *Environmental Science and Technology* 53: 4020–4029. https://doi.org/10.1021/acs.est.8b03655.

Celis-Hernandez, O., E. Ávila, J. Rendón-von Osten, E.A. Briceño-Vera, M.M. Borges-Ramírez, A.M. Gómez-Ponce, and V.M. Capparelli. 2023. Environmental risk of microplastics in a Mexican coastal lagoon ecosystem: Anthropogenic inputs and its possible human food risk. *Science of the Total Environment* 879: 163095. https://doi.org/10.1016/j.scitotenv.2023.163095.

Class, H., P. Bürkle, T. Sauerborn, O. Trötschler, B. Strauch, and M. Zimmer. 2021. On the role of density-driven dissolution of CO 2 in phreatic karst systems. *Water Resources Research*. https://doi.org/10.1029/2021WR030912.

Cohuo, S., A. Moreno-López, N.Y. Escamilla-Tut, A.M. Pérez-Tapia, I. Santos-Itzá, L.A. Macario-González, C.A. Villegas-Sánchez, and A. Medina-Quej. 2023. Assessment of water quality and heavy metal environmental risk on the peri-urban karst tropical Lake La Sabana. *Yucatán Peninsula. Water* 15: 390. https://doi.org/10.3390/w15030390.

Cole, J.J., Y.T. Prairie, N.F. Caraco, W.H. McDowell, L.J. Tranvik, R.G. Striegl, C.M. Duarte, et al. 2007. Plumbing the global carbon cycle: Integrating inland waters into the terrestrial carbon budget. *Ecosystems* 10: 172–185. https://doi.org/10.1007/s10021-006-9013-8.

CONANP. 1994. Laguna de Términos. Area de Protección de Flora y Fauna.

Culkin, F. 1965. The major constituents of seawater. *Chemical oceanography* 1. Academic Press pp 121–161.

David, L.T., and B. Kjerfve. 1998. Tides and currents in a two-inlet coastal lagoon: Laguna de Terminos, Mexico. *Continental Shelf Research* 18: 1057–1079. https://doi.org/10.1016/S0278-4343(98)00033-8.

Dickson, A.G., C.L. Sabine, and J.R. Christian. 2007. *Guide to best practices for ocean CO2 measurements*. *PICES Special Publication*. 3.

Doney, S.C., D.S. Busch, S.R. Cooley, and K.J. Kroeker. 2020. The impacts of ocean acidification on marine ecosystems and reliant human communities. *Annual Review of Environment and Resources.* 45: 83. https://doi.org/10.1146/annurev-environ-012320-083019.

Doney, S.C., V.J. Fabry, R.A. Feely, and J.A. Kleypas. 2009. Ocean acidification: The other CO 2 problem. *Annual Review of Marine Science* 1: 169–192. https://doi.org/10.1146/annurev.marine.010908.163834.

Dutta, M.K., S. Kumar, R. Mukherjee, P. Sanyal, and S.K. Mukhopadhyay. 2019. The post-monsoon carbon biogeochemistry of the Hooghly-Sundarbans estuarine system under different levels of anthropogenic impacts. *Biogeosciences* 16: 289–307. https://doi.org/10.5194/bg-16-289-2019.

Escobar-Toledo, F., M.J. Zetina-Rejón, J. Ramos-Miranda, and F. Arreguín-Sánchez. 2017. Temporal shifts in functional traits of the fish community in Terminos Lagoon (Mexico) in three

periods (1980, 1998 and 2011). *Environmental Biology of Fishes* 100: 1575–1586. https://doi.org/10.1007/s10641-017-0666-2.

Esparza, Contreras Ruiz, and A., P. Douillet, and J. Zavala-Hidalgo. 2014. Tidal dynamics of the Terminos Lagoon, Mexico: Observations and 3D numerical modelling. *Ocean Dynamics* 64: 1349–1371. https://doi.org/10.1007/s10236-014-0752-3.

Freitas, R., L. De Marchi, M. Bastos, A. Moreira, C. Velez, S. Chiesa, F.J. Wrona, E. Figueira, and A.M.V.M. Soares. 2017. Effects of seawater acidification and salinity alterations on metabolic, osmoregulation and oxidative stress markers in Mytilus galloprovincialis. *Ecological Indicators* 79: 54–62. https://doi.org/10.1016/j.ecolind.2017.04.003.

Fuentes-Yaco, C., D.A.S. de León, M.A. Monreal-Gómez, and F. Vera-Herrera. 2001. Environmental forcing in a tropical estuarine ecosystem: The Palizada River in the southern Gulf of Mexico. *Marine and Freshwater Research* 52: 735. https://doi.org/10.1071/MF00077.

García-Ríos, V., L. Alpuche-Gual, J. Herrera-Silveira, J. Montero-Muñoz, S. Morales-Ojeda, D. Pech, M.F. Cepeda-González, O. Zapata-Pérez, and G. Gold-Bouchot. 2013. Towards a coastal condition assessment and monitoring of the Gulf of Mexico Large Marine Ecosystem (GoM LME): Terminos Lagoon pilot site. *Environmental Development* 7: 72–79. https://doi.org/10.1016/j.envdev.2013.04.007.

Gaspar, F.L., B.R. Pinheiro, C.E.D. Noriega, M. Araujo, N. Lefèvre, and M. de J. F. Montes. 2018. Alkalinity, inorganic carbon and CO2 flux variability during extreme rainfall years (2010–2011) in two polluted tropical estuaries NE Brazil. *Brazilian Journal of Oceanography* 66: 115–130. https://doi.org/10.1590/s1679-87592018149406601.

Gomez, F.A., R. Wanninkhof, L. Barbero, S.-K. Lee, and F.J. Hernandez. 2020. Seasonal patterns of surface inorganic carbon system variables in the Gulf of Mexico inferred from a regional high-resolution ocean biogeochemical model. *Biogeosciences* 17: 1685–1700. https://doi.org/10.5194/bg-17-1685-2020.

Gonneea, M.E., M.A. Charette, Q. Liu, J.A. Herrera-Silveira, and S.M. Morales-Ojeda. 2014. Trace element geochemistry of groundwater in a karst subterranean estuary (Yucatan Peninsula, Mexico). *Geochimica Et Cosmochimica Acta* 132: 31–49. https://doi.org/10.1016/j.gca.2014.01.037.

Grenier, C., R. Román, C. Duarte, J.M. Navarro, A.B. Rodriguez-Navarro, and L. Ramajo. 2020. The combined effects of salinity and pH on shell biomineralization of the edible mussel Mytilus chilensis. *Environmental Pollution* 263: 114555. https://doi.org/10.1016/j.envpol.2020.114555.

Grenz, C., R. Fichez, C.Á. Silva, L.C. Benítez, P. Conan, A.C.R. Esparza, L. Denis, et al. 2017. Benthic ecology of tropical coastal lagoons: Environmental changes over the last decades in the Términos Lagoon. *Mexico* 349: 319–329.

Gunn, J.D., W.J. Folan, and H.R. Robichaux. 1995. A landscape analysis of the Candelaria watershed in Mexico: insights into paleoclimates affecting upland horticulture in the southern Yucatan Peninsula Semi-Karst. Geoarchaeology: An. *International Journal* 10: 3–42.

Guo, X., W.-J. Cai, W. Zhai, M. Dai, Y. Wang, and B. Chen. 2008. Seasonal variations in the inorganic carbon system in the Pearl River (Zhujiang) estuary. *Continental Shelf Research* 28: 1424–1434. https://doi.org/10.1016/j.csr.2007.07.011.

Han, Q., B. Wang, C.-Q. Liu, F. Wang, X. Peng, and X.-L. Liu. 2018. Carbon biogeochemical cycle is enhanced by damming in a karst river. *Science of the Total Environment* 616–617: 1181–1189. https://doi.org/10.1016/j.scitotenv.2017.10.202.

Hernández-Ayón, J.M., S.L. Belli, and A. Zirino. 1999. pH, alkalinity and total CO2 in coastal seawater by potentiometric titration with a difference derivative readout. Analytica Chimica Acta 394. Elsevier: 101–108. https://doi.org/10.1016/S0003-2670(99)00207-X.

Herrera-Silveira, J.A., A.L. Lara-Domínguez, J.W. Day, A. Yáñez-Arancibia, S.M. Ojeda, C.T. Hernández, and G.P. Kemp. 2019. *Ecosystem functioning and sustainable management in coastal systems with high freshwater input in the Southern Gulf of Mexico and Yucatan Peninsula*. *Coasts and Estuaries: The Future*. https://doi.org/10.1016/B978-0-12-814003-1.00022-8.

Hildebrand, A.R., G.T. Penfield, D.A. Kring, M. Pilkington, A. Camargo, Z.S.B. Jacobsen, and W.V. Boynton. 1991. Chicxulub Crater: A possible Cretaceous/Tertiary boundary impact crater on the Yucatán Peninsula. *Mexico. Geology* 19: 867. https://doi.org/10.1130/0091-7613(1991)019%3c0867:CCAPCT%3e2.3.CO;2.

Hoegh-Guldberg, O., P.J. Mumby, A.J. Hooten, R.S. Steneck, P. Greenfield, E. Gomez, C.D. Harvell, et al. 2007. Coral reefs under rapid climate change and ocean acidification. *Science* 318: 1737–1742. https://doi.org/10.1126/science.1152509.

Hofmann, M., S. Mathesius, E. Kriegler, D.P. van Vuuren, and H.J. Schellnhuber. 2019. Strong time dependence of ocean acidification mitigation by atmospheric carbon dioxide removal. *Nature Communications* 10: 5592. https://doi.org/10.1038/s41467-019-13586-4.

Hu, X., H. Yao, M.R. McCutcheon, L. Dias, C.J. Staryk, M.S. Wetz, and P.A. Montagna. 2022. Aragonite saturation states in estuaries along a climate gradient in the northwestern Gulf of Mexico. *Frontiers in Environmental Science* 10: 951256. https://doi.org/10.3389/fenvs.2022.951256.

Hudson, P. F., D. A. Hendrickson, A. C. Benke, A. Varela-Romero, R. Rodiles-Hernández, and W. L. Minckley. 2005. Rivers of Mexico. Rivers of North America. Academic Press: 1030–1084. https://doi.org/10.1016/B978-012088253-3/50026-2.

Humphreys, M.P., E.R. Lewis, J.D. Sharp, and D. Pierrot. 2022. PyCO2SYS v1.8: Marine carbonate system calculations in Python. *Geoscientific Model Development* 15: 15–43. https://doi.org/10.5194/gmd-15-15-2022.

INEGI. 2020. Censo de Población y Vivienda 2020.

IPCC. 2020. *Climate change: the IPCC response strategies*. *Climate change: the IPCC response strategies*.

Jaqueto, P., R.I.F. Trindade, J.M. Feinberg, J. Carmo, V.F. Novello, N.M. Stríkis, F.W. Cruz, M.H. Shimizu, and I. Karmann. 2021. Magnetic mineralogy of speleothems from tropical-subtropical sites of South America. *Frontiers in Earth Science* 9: 634482. https://doi.org/10.3389/feart.2021.634482.

Jiang, L.-Q., B.R. Carter, R.A. Feely, S.K. Lauvset, and A. Olsen. 2019. Surface ocean pH and buffer capacity: Past, present and future. *Scientific Reports* 9: 18624. https://doi.org/10.1038/s41598-019-55039-4.

Johnson, K.M., J.M. Sieburth, and P. J. leB Williams, and L. Brändström. 1987. Coulometric total carbon dioxide analysis for marine studies: Automation and calibration. *Marine Chemistry* 21: 117–133. https://doi.org/10.1016/0304-4203(87)90033-8.

Jupin, J.L.J., A.C. Ruiz-Fernández, A. Sifeddine, J.A. Sanchez-Cabeza, L.H. Pérez-Bernal, J.G. Cardoso-Mohedano, M.A. Gómez-Ponce, and J.G. Flores-Trujillo. 2023. Anthropogenic drivers of increasing sediment accumulation in contrasting Mexican mangrove ecosystems. *CATENA* 226: 107037. https://doi.org/10.1016/j.catena.2023.107037.

Kibria, G., D. Nugegoda, G. Rose, and A.K.Y. Haroon. 2021. Climate change impacts on pollutants mobilization and interactive effects of climate change and pollutants on toxicity and bioaccumulation of pollutants in estuarine and marine biota and linkage to seafood security. *Marine Pollution Bulletin* 167: 112364. https://doi.org/10.1016/j.marpolbul.2021.112364.

Lee, D.Y., M.S. Owens, M. Doherty, E.M. Eggleston, I. Hewson, B.C. Crump, and J.C. Cornwell. 2015. The Effects of Oxygen

Transition on Community Respiration and Potential Chemoautotrophic Production in a Seasonally Stratified Anoxic Estuary. *Estuaries and Coasts* 38: 104–117. https://doi.org/10.1007/s12237-014-9803-8.

Lewis, E.R., and D.W.R. Wallace. 1998. Program Developed for CO2 System Calculations. [object Object]. https://doi.org/10.15485/1464255.

Liu, J., E. Hrustić, J. Du, B. Gašparović, M. Čanković, N. Cukrov, Z. Zhu, and R. Zhang. 2019. Net Submarine Groundwater-Derived Dissolved Inorganic Nutrients and Carbon Input to the Oligotrophic Stratified Karstic Estuary of the Krka River (Adriatic Sea, Croatia). *Journal of Geophysical Research: Oceans* 124: 4334–4349. https://doi.org/10.1029/2018JC014814.

Liu, T., H. Nie, J. Ding, Z. Huo, and X. Yan. 2024. Physiological and transcriptomic analysis provides new insights into osmoregulation mechanism of Ruditapes philippinarum under low and high salinity stress. *Science of The Total Environment*. https://doi.org/10.1016/j.scitotenv.2024.173215.

Machain-Castillo, M.L., A.C. Ruiz-Fernández, R. Alonso-Rodríguez, J.A. Sanchez-Cabeza, F.R. Gío-Argáez, A. Rodríguez-Ramírez, R. Villegas-Hernández, et al. 2020. Anthropogenic and natural impacts in the marine area of influence of the Grijalva – Usumacinta River (Southern Gulf of Mexico) during the last 45 years. *Marine Pollution Bulletin* 156: 111245. https://doi.org/10.1016/j.marpolbul.2020.111245.

McDougall, T.J., and P.M. Barker. 2011. *Getting started with TEOS-10 and the gibbs seawater (GSW) oceanographic toolbox*. SCOR/IAPSO WG127.

McGrath, T., E. McGovern, C. Gregory, and R.R. Cave. 2019. Local drivers of the seasonal carbonate cycle across four contrasting coastal systems. *Regional Studies in Marine Science* 30: 100733. https://doi.org/10.1016/j.rsma.2019.100733.

Medina-Gómez, I., G. Villalobos-Zapata, and J.A. Herrera-Silveira. 2015. Spatial and Temporal Hydrological Variations in the Inner Estuaries of a Large Coastal Lagoon of the Southern Gulf of Mexico. *Journal of Coastal Research* 31: 1429–1438. https://doi.org/10.2112/JCOASTRES-D-13-00226.1.

Merino, M. 1997. Upwelling on the Yucatan Shelf: Hydrographic evidence. *Journal of Marine Systems* 13: 101–121. https://doi.org/10.1016/S0924-7963(96)00123-6.

Millero, F.J. 2010. Carbonate constants for estuarine waters. *Marine and Freshwater Research* 61: 139. https://doi.org/10.1071/MF09254.

Moreno-Pérez, P.A., M. Hernández-Téllez, and A. Bautista-Gálvez. 2021. In Danger One of the Largest Aquifers in the World, the Great Mayan Aquifer, Based on Monitoring the Cenotes of the Yucatan Peninsula. *Archives of Environmental Contamination and Toxicology* 81: 189–198. https://doi.org/10.1007/s00244-021-00869-5.

Mucci, A. 1983. The solubility of calcite and aragonite in seawater at various salinities, temperatures, and one atmosphere total pressure. *American Journal of Science* 283: 780–799. https://doi.org/10.2475/ajs.283.7.780.

Ocaña, D., and A. Lot. 1996. Estudio de la vegetación acuática vascular del sistema fluvio-lagunar-deltáico del río Palizada, Campeche, México. *Anales Del Instituto De Biología, Universidad Nacional Autónoma De México* 67: 303–327.

Orr, J.C., J.-M. Epitalon, A.G. Dickson, and J.-P. Gattuso. 2018. Routine uncertainty propagation for the marine carbon dioxide system. *Marine Chemistry* 207: 84–107. https://doi.org/10.1016/j.marchem.2018.10.006.

Orr, J.C., V.J. Fabry, O. Aumont, L. Bopp, S.C. Doney, R.A. Feely, A. Gnanadesikan, et al. 2005. Anthropogenic ocean acidification over the twenty-first century and its impact on calcifying organisms. *Nature* 437: 681–686. https://doi.org/10.1038/nature04095.

Osborne, E., X. Hu, E.R. Hall, K. Yates, J. Vreeland-Dawson, K. Shamberger, L. Barbero, et al. 2022. Ocean acidification in the Gulf of Mexico: Drivers, impacts, and unknowns. *Progress in Oceanography* 209: 102882. https://doi.org/10.1016/j.pocean.2022.102882.

Pain, A.J., J.B. Martin, C.R. Young, A. Valle-Levinson, and I. Mariño-Tapia. 2020. Carbon and phosphorus processing in a carbonate karst aquifer and delivery to the coastal ocean. *Geochimica Et Cosmochimica Acta* 269: 484–495. https://doi.org/10.1016/j.gca.2019.10.040.

Perry, E., G. Velazquez-Oliman, and L. Marin. 2002. The Hydrogeochemistry of the Karst Aquifer System of the Northern Yucatan Peninsula, Mexico. *International Geology Review* 44: 191–221. https://doi.org/10.2747/0020-6814.44.3.191.

Phleger, F.B., and A. Ayala. 1971. Processes and History of Terminos Lagoon, Mexico. AAPG Bulletin 55. https://doi.org/10.1306/819A3E26-16C5-11D7-8645000102C1865D.

Queb-Suarez, J.E., A. Ruiz-Marin, Y. Canedo-Lopez, C.A. Aguilar-Ucan, C. Montalvo-Romero, J.G. Flores-Trujillo, and N. Perez-Morga. 2022. Source Identification, Toxicity, and Persistence of PAHs in Sediment Core from a Natural Protected Area in Mexico. *Energies* 15: 7116. https://doi.org/10.3390/en15197116.

Ramos, E.L. 1975. Geological Summary of the Yucatan Peninsula. In *The Gulf of Mexico and the Caribbean*, 257–282. Boston, MA: Springer US. https://doi.org/10.1007/978-1-4684-8535-6_7.

Ramsar. 2004. Área de Protección de Flora y Fauna Laguna de Términos. *1356*.

Raymond, P.A., and S.K. Hamilton. 2018. Anthropogenic influences on riverine fluxes of dissolved inorganic carbon to the oceans. *Limnology and Oceanography Letters* 3: 2378–2242. https://doi.org/10.1002/lol2.10069.

Raymond, P.A., J. Hartmann, R. Lauerwald, S. Sobek, C. McDonald, M. Hoover, D. Butman, et al. 2013. Global carbon dioxide emissions from inland waters. *Nature* 503: 355–359. https://doi.org/10.1038/nature12760.

Reyes, E., and M. Merino. 1991. Diel dissolved oxygen dynamics and eutrophication in a shallow, well-mixed tropical lagoon (Cancun, Mexico). *Estuaries* 14: 372–381. https://doi.org/10.2307/1352262.

Rosentreter, J.A., and B.D. Eyre. 2020. Alkalinity and dissolved inorganic carbon exports from tropical and subtropical river catchments discharging to the Great Barrier Reef, Australia. *Hydrological Processes* 34: 1530–1544. https://doi.org/10.1002/hyp.13679.

Ruiz-Fernández, A.C., J.A. Sanchez-Cabeza, T. Cuéllar-Martínez, L.H. Pérez-Bernal, V. Carnero-Bravo, E. Ávila, and J.G. Cardoso-Mohedano. 2020. Increasing salinization and organic carbon burial rates in seagrass meadows from an anthropogenically-modified coastal lagoon in southern Gulf of Mexico. *Estuarine, Coastal and Shelf Science* 242: 106843. https://doi.org/10.1016/j.ecss.2020.106843. Academic Press: 106843.

Sarma, V.V.S.S., M.S. Krishna, V.D. Rao, R. Viswanadham, N.A. Kumar, T.R. Kumari, L. Gawade, S. Ghatkar, and A. Tari. 2012. Sources and sinks of CO2 in the west coast of Bay of Bengal. *Tellus b: Chemical and Physical Meteorology* 64: 10961. https://doi.org/10.3402/tellusb.v64i0.10961.

Seabold, S., and J. Perktold. 2010. Statsmodels: Econometric and statistical modeling with python. In *9th Python in Science Conference*.

Smith, V. H., G.D. Tilman, and J.C. Nekola. 1999. Eutrophication: Impacts of excess nutrient inputs on freshwater, marine, and terrestrial ecosystems. In *Environmental Pollution*, 100:179–196. Elsevier Ltd. https://doi.org/10.1016/S0269-7491(99)00091-3.

Sosa-López, A., D. Mouillot, J. Ramos-Miranda, D. Flores-Hernandez, and T. Do Chi. 2006. Fish species richness decreases with salinity in tropical coastal lagoons. *Journal of Biogeography* 34: 52–61. https://doi.org/10.1111/j.1365-2699.2006.01588.x.

Takahashi, T., W. S. Broecker, and A. E. Bainbridge, ed. 1982. *GEOSECS pacific expedition volume 3, hydrographic data 1973–1974*. National Science Foundation.

Taminskas, J., R. Paskauskas, A. Zvikas, and J. Satkunas. 2006. Karst and Ecosystems. In *Geology and Ecosystems*, 61–76. Boston, MA: Springer US. https://doi.org/10.1007/0-387-29293-4_6.

Vazquez, F., R. Rangel, A.M. Quintero-Marmol, J. Fernandez, E. Aguayo, A. Palacio, and V. K. Sharma. 2000. *Southern Gulf of Mexico. Seas at the millennium - an environmental evaluation - Volume 1*.

Vazquez, G., V.K. Sharma, V.R. Magallanes, and A.J. Marmolejo. 1999. Heavy Metals in a Coastal Lagoon of the Gulf of Mexico. *Marine Pollution Bulletin* 38: 479–485. https://doi.org/10.1016/S0025-326X(98)00173-8.

Vinebrooke, R., K. Cottingham, J. Marten Scheffer, S. Dodson, S. Maberly, and U. Sommer. 2004. Impacts of multiple stressors on biodiversity and ecosystem functioning: The role of species co-tolerance. *Oikos* 104: 451–457. https://doi.org/10.1111/j.0030-1299.2004.13255.x.

Virtanen, P., R. Gommers, T.E. Oliphant, M. Haberland, T. Reddy, D. Cournapeau, E. Burovski, et al. 2020. SciPy 1.0: Fundamental algorithms for scientific computing in Python. *Nature Methods* 17: 261–272. https://doi.org/10.1038/s41592-019-0686-2.

Volta, C., D.T. Ho, D.T. Maher, R. Wanninkhof, G. Friederich, C. Del Castillo, and H. Dulai. 2020. Seasonal Variations in Dissolved Carbon Inventory and Fluxes in a Mangrove-Dominated Estuary. *Global Biogeochemical Cycles* 34. https://doi.org/10.1029/2019GB006515.

Wallace, R.B., H. Baumann, J.S. Grear, R.C. Aller, and C.J. Gobler. 2014. Coastal ocean acidification: The other eutrophication problem. *Estuarine, Coastal and Shelf Science* 148: 1–13. https://doi.org/10.1016/j.ecss.2014.05.027.

Wang, Z.A., R. Wanninkhof, W.-J. Cai, R.H. Byrne, X. Hu, T.-H. Peng, and W.-J. Huang. 2013. The marine inorganic carbon system along the Gulf of Mexico and Atlantic coasts of the United States: Insights from a transregional coastal carbon study. *Limnology and Oceanography* 58: 325–342. https://doi.org/10.4319/lo.2013.58.1.0325.

Xue, L., and W.-J. Cai. 2020. Total alkalinity minus dissolved inorganic carbon as a proxy for deciphering ocean acidification mechanisms. *Marine Chemistry* 222: 103791. https://doi.org/10.1016/j.marchem.2020.103791.

Xue, L., W.-J. Cai, T. Takahashi, L. Gao, R. Wanninkhof, M. Wei, K. Li, L. Feng, and W. Yu. 2018. Climatic modulation of surface acidification rates through summertime wind forcing in the Southern Ocean. *Nature Communications* 9: 3240. https://doi.org/10.1038/s41467-018-05443-7.

Yáñez-Arancibia & Day, Jr. 1982. Ecological characterization of Terminos Lagoon, a tropical lagoon-estuarine system in the Gulf of Mexico. *Oceanologica Acta* 5 (suppl.): 431–450.

Yang, B., R.H. Byrne, and M. Lindemuth. 2015. Contributions of organic alkalinity to total alkalinity in coastal waters: A spectrophotometric approach. *Marine Chemistry* 176: 199–207. https://doi.org/10.1016/j.marchem.2015.09.008.

YSI. 2020. EXO User Manual: Advanced Water Quality Monitoring Platform (Revision K). https://www.ysi.com/EXO

Zhong, J., S. Li, F. Tao, F. Yue, and C.-Q. Liu. 2017. Sensitivity of chemical weathering and dissolved carbon dynamics to hydrological conditions in a typical karst river. *Scientific Reports* 7: 42944. https://doi.org/10.1038/srep42944.

Zopfi, J., T.G. Ferdelman, B.B. Jørgensen, A. Teske, and B. Thamdrup. 2001. Influence of water column dynamics on sulfide oxidation and other major biogeochemical processes in the chemocline of Mariager Fjord (Denmark). *Marine Chemistry* 74: 29–51. https://doi.org/10.1016/S0304-4203(00)00091-8.